

CHARACTERISTICS OF A PLASMATRON WITH AN INSERT BETWEEN THE ELECTRODES

G. Yu. Dautov, Yu. S. Dudnikov, M. F. Zhukov, G. M. Mustafin, and M. I. Sazonov

Zhurnal Prikladnoi, Mekhaniki i Teoreticheskoi Fiziki, Vol. 8, No. 1, pp. 172-176, 1967

Electrical and thermal characteristics are presented for a plasma torch with a sectional insert between the electrodes; these are compared with the characteristics of a single-chamber source. The voltage-current curves have a minimum, the voltage on the rising branch being higher than that for a single-chamber torch. The voltage and brightness fluctuations are much lower than those for a single-chamber torch.

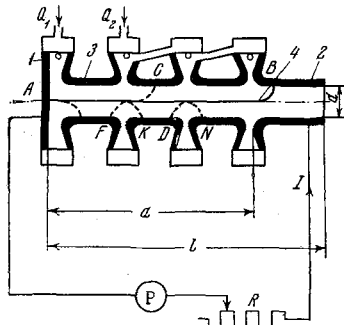


Fig. 1. Section of the arc chamber; 1) cathode, 2) anode, 3) insert, 4) arc; G_1 and G_2 are the air inlets, P is the power supply, R is the resistor.

1. Some aspects of an arc in a segmented channel. The stabilized arc in a plasma torch interacts electrically and thermally with the flow of hot gas and with the channel wall. The hot gas usually fills the tube completely in a laminar or cylindrical arc, the arc interacting directly with the wall and being stabilized by the latter. The length and potential difference of such an arc may be increased by inserting short sections insulated from the electrodes and from one another [1]. If the arc is to burn normally along the axis of the tube, the potential difference across one section should not exceed the sum of the cathode and anode potential differences characteristic of an

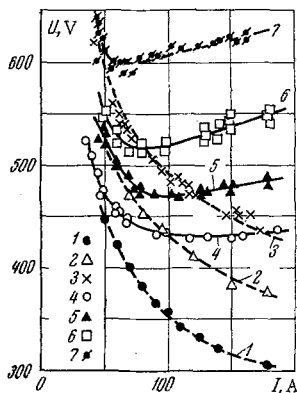


Fig. 2. U-I curves for $d = 1$ cm, $p = 10$ N/cm²: 1) $G = 6$ g/sec, $n = 6$, $l = 17.7$ cm, sections connected electrically to anode; 2) single-chamber source, $G = 6$, $l = 30$; 3) as previous, $G = 8$, $l = 30$; 4) $G = 6$, $n = 6$, $a = 12$ cm, $l = 17.7$; 5) $G = 8$, $n = 6$, $a = 12.6$, $l = 17.7$; 6) $G = 8$, $n = 7$, $a = 14.7$, $l = 19.8$; 7) $G = 8$, $n = 8$, $a = 16.9$, $l = 22$.

arc discharge under these conditions. Vigorous wall cooling is essential to long-term working, while the state of the surface greatly

affects the electrical processes near the wall [2]. Such devices have been operated at low gas flow rates, have very low thermal efficiencies, and are used mainly for research purposes.

The gas flow plays an increasing part in the interactions as the flow rate increases, and the flow allows the arc to be stabilized at the axis (vortex stabilization) while providing a substantial increase in length, voltage, power, and efficiency. However, there are [3-6] limits to the increase in length and power, on account of shunting of the arc to the wall. The arc characteristics may be adjusted in this case by the use of inserts [7, 8]; one-section inserts have been used [5, 7-9], but a study of the mode of operation [9] shows that it is better to use several insert sections, with a supply of cold gas between them.

Such a device differs essentially from the channel in a laminar or cylindrical arc in that arcs of FK and DN types (Fig. 1) may be formed between adjacent sections in accordance with the potential for arc breakdown between the arc column and the sections, and also with the potential for breakdown between sections. These potentials may be much greater than the sum of the cathode and anode potential differences, so the individual sections may be much longer than in a laminar or cylindrical arc if the arc has its normal position at the axis of the channel. Gas supply to the gaps provides control of the breakdown potentials and prevents formation of short arcs on the gaps.

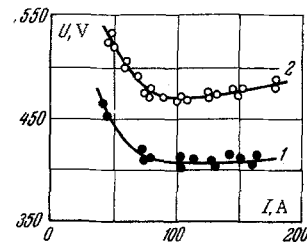


Fig. 3. U-I curves for a plasma jet with sections, $d = 1$ cm, $p = 10$ N/cm², $n = 6$, $a = 12.6$, $l = 17.7$ cm, G of: 1) 5, 2) 8.

The main gas flow rate is heated as it moves along the channel, but the layer of cold gas at the wall maintains the difference in performance up to large currents and lengths.

Tests [10] show that a section becomes charged to the potential of some point in the positive column by leakage between the arc column and the section; the maximum potential difference between the arc and a section becomes much less than that for an undivided insert of the same length. Current leakage from the sections may occur if these are water-cooled, as in high-power jets. There is little leakage between arc column and section if the layer of cold gas is thick [9], and so it is possible for the potential difference between the column and a section to become sufficient for breakdown. In that case the potentials may be equalized by connecting the section to an appropriate voltage source.

It has been shown [10] that the gas flow rate has little effect on the field E in an arc with vortex stabilization, so we expect that a sectional insert and gas injection between sections will together provide not only increase in length but also in arc burning voltage, in conjunction with high efficiency. Here we consider the characteristics of a simple plasma jet of this type.

Interactions near the electrode wall play a large part in a two-chamber jet and in a jet with bilateral efflux, so it is possible that the results given here will assist in improving the characteristics of such devices.

2. Apparatus. Figure 1 shows the system. The copper cathode 1, anode 2, and insulated sections 3 are cooled by water. The number n of the sections (each 2 cm long) varied from five to eight, so the interelectrode distance a varied correspondingly from 10.5 to 16.9 cm, while the length l of the arc chamber (distance from the end face of the cathode to the exit end of the anode) ranged from 15.5 to 22 cm. Anode 2 had a fixed length $l_2 = 5$ cm.

Air (flow rate G_1) enters the 3.5 mm gap between the cathode and the first section via four tangential holes 3 mm in diameter at a distance of 2.5 cm from the axis. Further gas (flow rate G_2) enters the spaces between sections via tangential holes and is distributed via the 1 mm gaps between sections in the arc chamber; $G = G_1 + G_2$ ranged from 5 to 8 g/sec. The arc was struck by the method previously described [9], and it then took up position AB. The tests were done with $g = G_2/G = 0.58$ for a system with an internal electrode diameter $d = 1$ cm. The gas was released into the atmosphere ($p = 10$ N/cm²). The temperature of the cooling water was read by a mercury thermometer with 0.5°C divisions; the water and air flow rates were monitored by RS-5 and RS-7 rotameters. The potential U and current I were recorded by E59 and LM-1 instruments, respectively, accuracy class 0.5.

3. Voltage-current curves. Figures 2 and 3 show the U-I curves. The multiple sections and supply of gas along the length substantially increase the burning voltage; the curve rises above a certain I . For example, curves 3 and 7 of Fig. 2 show that U is about 40% higher than for a single-chamber jet (continuous anode) for $I = 150$ A, $n = 8$, and $G = 8$ g/sec.

If section 3 is connected electrically to the anode 2, the two together act as a sectional anode with distributed gas supply. Comparison of curves 1 and 2 (continuous anode) shows that a sectional anode with distributed supply gives lower U for a given G than a single-chamber jet with a continuous anode, e.g., 20% less for $I = 150$ A and $G = 6$ g/sec. The effect for large I occurs because the arc takes up the position AC (Fig. 1) in the sectional case, and part of the gas enters downstream from C, i.e., takes no part in blowing the arc; however, the arc at low I lies in position AB, and all the incoming gas participates in blowing the arc, but with U remaining less than for a single-chamber device. This means that there must be other reasons for the reduction in U . One of these may be perturbations in the distribution of velocities (and hence temperatures) on account of the slots in the electrode, which influence the interactions near the wall, with the consequence of earlier shunting and hence shorter arcs. This effect can occur at low I when the sections are insulated from the anode; but, in that case, U is not so greatly reduced, because shunting to a part of the inserts is impossible (curves 2 and 4), and hence the scale of the shunting is reduced. This reduction in U is

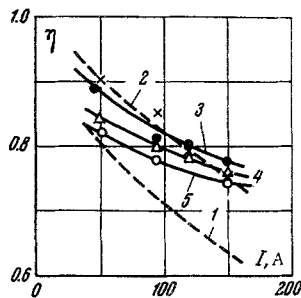


Fig. 4. Relation of η to I for $G = 6$ g/sec, $d = 1$ cm, and $p = 10$ N/cm²: 1) continuous anode, $l = 30$ cm (calculated curve); 2) continuous anode, $l = 17.7$; 3) $n = 6$, $a = 12.6$, $l = 17.7$; 4) $n = 7$, $a = 14.7$, $l = 19.8$; 5) $n = 8$, $a = 16.9$, $l = 22$.

rapidly lost as I and a increase. The arc length in the present device at large I exceeds the length in a single-chamber device with a continuous anode, so U is higher and the U-I curve rises. The increase in U itself increases with the length, as curves 5-7 of Fig. 2 show.

The rise in the U-I curve for the present device does not have the same cause as that rise for a cylindrical arc; in the latter case, the rise cannot start until the arc completely fills the cross-section [11], after which point the total conductivity can increase with I only as a result of increase in T , which is less rapid than the increase in I , so the U-I curve rises. In the present device, the rise in the U-I curve begins long before the arc fills the channel; here there is a substantial cold layer of vortex flow between the arc and the wall, and the U-I curve rises because the E-I curve passes through a minimum (E is field strength) for a column under these conditions [10]. This is a substantial difference between the present device and a sectional channel in a cylindrical or laminar arc. It is to be expected that the present device will also show effects on the U-I curve from geometrical limitation of the arc at high I .

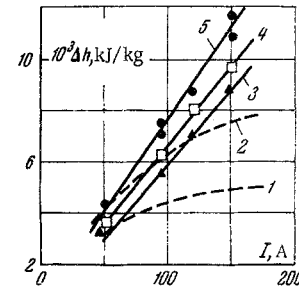


Fig. 5. Increase in retardation enthalpy for air in a plasma jet, $G = 6$ g/sec, $d = 1$ cm, $p = 10$ N/cm²: 1) continuous anode, $l = 30$; 2) continuous anode, $l = 17.7$; 3) $n = 6$, $a = 12.6$, $l = 17.7$; 4) $n = 7$, $a = 14.7$, $l = 19.8$; 5) $n = 8$, $a = 16.9$, $l = 22$.

The positive slope of the U-I curve is of considerable significance as regards improving the over-all efficiency by eliminating the stabilizing ballast resistor in the line from a source of low or very low internal resistance. Moreover, increase in U means that lower I are needed for a given power, which provides more reserve in the device.

4. Thermal characteristics. The good arc length stability in the present device, together with the screening action of the incoming gas, causes the thermal efficiency η as a function of I to differ somewhat from that for a single-chamber device. The solid lines in Fig. 4 show η as a function of I for three lengths, while the dashed lines show the curves for a single-chamber device. Curve 2 is from experiment for $l = 18$ cm, while curve 1 has been calculated for $l = 30$ cm from the equation of [12]

$$\eta = -1 + \frac{2.52}{(pd)^{0.05}} - 0.17 \lg \frac{I^2}{Gd}$$

The maximal arc length l_{arc} (length in the axial direction) in a device without sections is very much dependent on I , and so the device of optimal η must have an adjustable length; if $l > l_{arc}$, the part $l_1 = l - l_{arc}$ serves only as a source of loss. Curves 1 and 2 are for constant l . Part of the arc emerged from the anode at small I in the experiments with $l = 18$ cm, so curve 2 for low I gives η in excess of the maximum possible value η_{max} . Curve 1 corresponds to $l > l_{arc}$ for all I , so η is everywhere less than η_{max} . The $\eta_{max} = f(I)$ curve for small I should lie between curves 1 and 2, approaching curve 1 as I increases. Curves 1 and 2 together show that the losses in l_1 are considerable. In the case of the present device, the anode length l_{arc} is excessive for large I , so there is a loss part l_1 , and curves 3-5 are also not optimal. Hence the $\eta_{max} = f_2(I)$ curve should lie somewhat above these curves.

The curves of Fig. 4 show that η for the present device exceeds that for a one-chamber device at high I , on account of the screening action and of the difference in the l_1 . Moreover, the present device can work without a ballast resistor at these currents, so the overall efficiency is considerably higher.

The Δh - I curves of Fig. 5 reveal most clearly the difference from a one-chamber device. Curves 1 and 2 are for a one-chamber

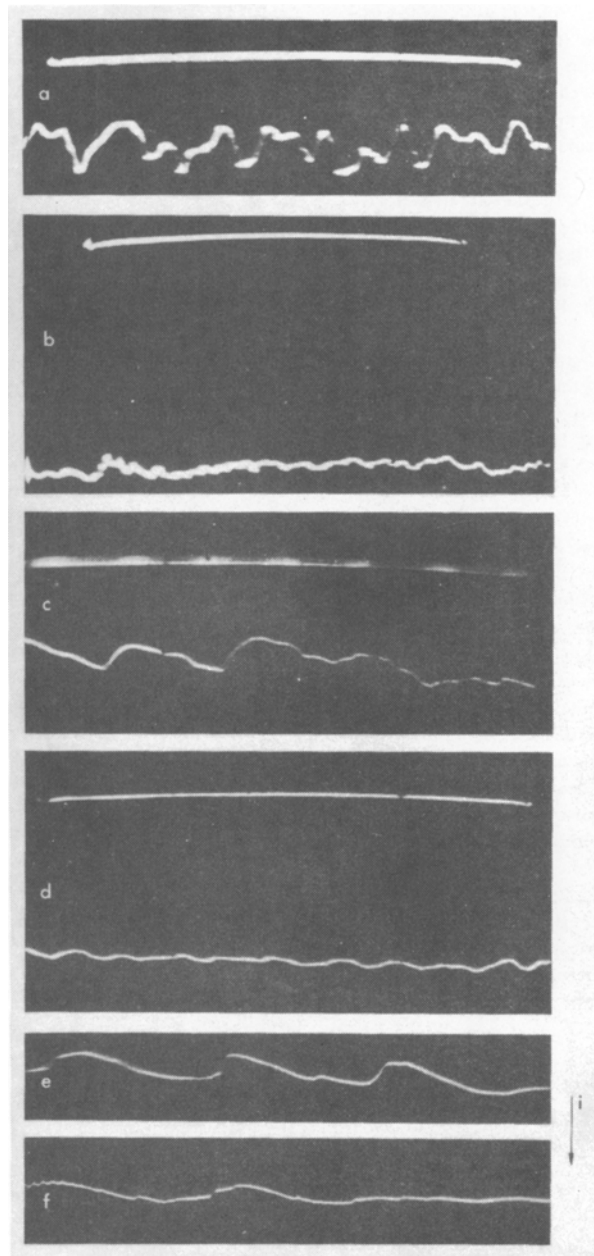


Fig. 6. Current and emission intensity at $I = 150$ A, $p = 10$ N/cm². Intensity: a) continuous anode, $G = 6.1$ g/sec, $U = 336$ V, sweep duration $\tau = 4.2$ msec; b) $n = 7$, $a = 14.7$ cm, $G = 6$, $U = 505$ V, $\tau = 4.6$ msec. Voltage: c) continuous anode, $G = 6$, $U = 360$ V, $\tau = 1.3$ msec; d) $n = 7$, $a = 14.7$, $G = 5.9$; $U = 505$ V, $\tau = 1.3$ msec; e) $n = 7$, $a = 14.7$, $G = 5.9$; $U = 510$ V, $\tau = 26$ μ sec; f) $n = 8$, $a = 16.9$, $G = 5.8$, $U = 585$ V, $\tau = 28$ μ sec.

device; in this case, the increase in l_1 for a given l causes the curves to tend towards limiting values, the limit occurring when the increase in power input via the arc equals the increase in power lost in l_1 . The limit becomes lower as l increases. The present device shows no such limit for I up to 150 A, Δh increasing linearly with I (and also with l). For instance, Δh for $I = 150$ A, $G = 6$ g/sec, and $a = 16.9$ cm exceeds by 45 and 100%, respectively, the values for a single-chamber device with l of 18 and 30 cm.

The present device thus not only realizes the advantages of section 3 but also provides access to higher T for a given l .

5. Fluctuations. Shunting causes fluctuations in U , T , and arc power; such fluctuations in jet parameters are undesirable in certain technical applications [13]. It is to be expected that the rising U - I curves for the present device will substantially reduce the scale of the fluctuations, while increasing the frequency, since shunting cannot occur within the sections, while T is increased near the anode.

We recorded oscillograms of U and the emission intensity at 8-9 mm from the far end of the anode in the present device and in a single-chamber device; an FEU-19 photomultiplier was used with ENO-1 and OK-17M oscilloscopes. Figure 6 shows the results, in which the upper lines correspond to zero signal (these lines are recorded as curves on photographing the curved screen of the ENO-1). Curves e and f represent the ac component of U recorded with the OK-17M.

The one-chamber device shows variations in U of up to 40% of the mean value (50% in the intensity), the frequency being several kHz. The present device showed about 8% variation in U and intensity, the frequency being about 10^5 Hz.

The present device can thus work without large variations in U and T on account of shunting. The variations become smoother (Fig. 6f) as I and l increase, i.e., as T in the shunting zone increases, and it is clear that the usual concept of large-scale shunting becomes inapplicable here.

REFERENCES

1. H. Maecker, Messung und Auswertung von Bogencharakteristiken (Ar, N₂), Z. Phys., vol. 4, no. 158, 1960.

2. H. B. Mckee, R. C. Dean, and A. Pytte, "On cooled anodes in contact with a laminar arc-heated flow," IEEE Trans. nucl. sci., VNS-11, no. 1, 1964.

3. Harvey, Simpkins, and Adcock, "Instability of arc columns," Raketnaya Tekhnika i Kosmonavtika, 1, no. 3, 1963.

4. H. Tareno, K. Saito, Anodic Phenomena in Nitrogen Plasma Jet. Japan. J. Appl. Phys., vol. 2, no. 3, 1963.

5. G. Yu. Dautov and M. F. Zhukov, "Some generalizations from arc studies," PMTF [Journal of Applied Mechanics and Technical Physics], no. 2, 1965.

6. V. Ya. Smolyakov, "Some aspects of the behavior of the arc in a dc plasma source," PMTF, no. 6, 1963.

7. A. V. Nikolaev and I. D. Kulagin, "Applications of an arc plasma torch," Vopr. Elekt., Ser. 1, no. 9, 1960.

8. W. Neumann, Charakteristiken von Argon-Plasmastrahlerzeugern für Unterschallgeschwindigkeit, Exp. Techn. Phys., vol. 2, 1962.

9. G. Yu. Dautov, Yu. S. Dudnikov, and M. I. Sazonov, "A study of a plasma source with an insert between the electrodes," Izv. SO AN SSSR, Ser. Tekh. Nauk, issue 3, no. 10, 1965.

10. G. Yu. Dautov, Yu. S. Dudnikov, M. F. Zhukov, and M. I. Sazonov, "Potential distribution along the arc in a vortex-type plasma torch," PMTF [Journal of Applied Mechanics and Technical Physics], no. 5, 1965.

11. G. M. Tikhodeev, Energy Aspects of a Welding Arc [in Russian], Izd. AN SSSR, 1961.

12. G. Yu. Dautov and M. F. Zhukov, "Dimensionless relationships for the characteristics of dc plasma torches," PMTF [Journal of Applied Mechanics and Technical Physics] no. 6, 1965.

13. V. O. German and M. G. Morozov, "Some results on a dc plasma torch," Teplofizika Vysokikh Temperatur, 2, no. 5, 1965.

29 December 1965

Novosibirsk